RESEARCH ARTICLE

# Modern stromatolite phototrophic communities: a comparative study of procaryote and eucaryote phototrophs using variable chlorophyll fluorescence

Rupert G. Perkins[1], Jean-Luc Mouget[2], Jacco C. Kromkamp[3], John Stolz[4] & R. Pamela Reid[5]

[1]School of Earth and Ocean and Sciences, Cardiff University, Cardiff, UK; [2]Ecophysiologie et métabolisme des microalgues, EA 2160 Mer-Molécules-Santé (MMS), Faculté des Sciences et Techniques, Université du Maine, Le Mans, France; [3]Royal Netherlands Institute of Sea Research (NIOZ), Yerseke, The Netherlands; [4]Department of Biological Sciences, Duquesne University, Pittsburgh, PA, USA; and [5]RSMAS/MGG, University of Miami, Miami, FL, USA

**Correspondence:** Rupert G. Perkins, School of Earth and Ocean and Sciences, Cardiff University, Cardiff CF10 3YE, UK. Tel.: +44 2920 875026; fax: +44 2920 875346; e-mail: perkinsr@cf.ac.uk

Received 2 February 2012; revised 23 May 2012; accepted 30 May 2012.

DOI: 10.1111/j.1574-6941.2012.01421.x

Editor: Gary King

**Keywords**
stromatolite; fluorescence; productivity; cyanobacteria; diatoms.

## Abstract

Stromatolites are laminated organosedimentary structures formed by microbial communities, principally cyanobacteria although eucaryote phototrophs may also be involved in the construction of modern stromatolites. In this study, productivity and photophysiology of communities from stromatolites (laminated) and thrombolites (nonlaminated) were analysed using fluorescence imaging. Sub-samples of mats were excised at Highborne Cay, Bahamas, and cross-sectioned to simultaneously analyse surface, near-surface (1–2 mm), and deeper (2–10 mm) communities. Rapid light curve parameters and nonphotochemical downregulation showed distinct differences between phototroph communities, consistent with the reported quasi-succession of classic stromatolite mat types. Greater productivity was shown by cyanobacteria in Type 1 and Type 3 mats (first and final stage of the succession, *Schizothrix gebeleinii* and *Solentia* sp. respectively) and lower productivity within Type 2 mats (intermediate mat type). Eucaryote mat types, dominated by stalked (*Striatella* sp. and *Licmophora* sp.) and tube-dwelling (e.g. *Nitzschia* and *Navicula* spp.) diatoms, showed greater productivity than cyanobacteria communities, with the exception of *Striatella* (low productivity) and an unidentified coccoid cyanobacterium (high productivity). Findings indicate comparative variability between photosynthetically active procaryote and eucaryote sub-communities within stromatolites, with a pattern logically following the succession of 'classic' mat types, and lower than the productivity of eucaryote dominated 'nonclassic' mat types.

## Introduction

Modern stromatolites are living examples of laminated microbial structures that have been present on the planet for over 80% of Earth history (Reid *et al.*, 2000; Riding, 2000; Visscher *et al.*, 2000). The margins of Exuma Sound, Bahamas, host the only known examples of modern stromatolites growing in open marine conditions, similar to those of many Precambrian platforms (Reid *et al.*, 1995, 1999). These living structures enable the study of interactions between phototrophic cyanobacteria and heterotrophic bacteria in the biostabilization of carbonate sand grains, biogenic precipitation of calcium carbonate, and resultant accretion of stromatolite lamina (Reid *et al.*, 2000). Thrombolites are similar in many respects to stromatolites, but lack the lamina structure and are characterized by a macroscopic clotted fabric (Shapiro, 2000).

Early work by Reid *et al.* (2000), at Highborne Cay, Exuma Sound, described three distinct microbial communities forming modern marine stromatolites. These communities, referred to as Mat Types 1, 2 and 3, show a quasi-succession from a pioneer community of filamentous cyanobacteria, mainly *Schizothrix gebeleinii,* which form unlithified layers of trapped and bound sediment





FEMS MICROBIOLOGY ECOLOGY

(Type 1), to biofilm mats dominated by sulphate reducing bacteria which form thin crusts of microcrystalline carbonate (Type 2), to a climax community dominated by the coccoid endolithic cyanobacterium *Solentia* sp. which create cemented layers of fused sand grains (Type 3). Stromatolite laminae form by a cycling of these communities with each subsurface layer representing a former surface mat. Stolz *et al.* (2009) expanded the study of 'classic' mat types described by Reid *et al.* (2000) to include the following trapping and binding communities: bacterial mats dominated by the filamentous cyanobacteria *Phormidium* sp., which form pudding-like mounds, and diatom mats dominated by either stalked diatoms, *Striatella unipunctata* and *Licmophora* spp., or tube-dwelling Naviculid diatoms.

Although a variety of microbial communities have been described on the surfaces of modern marine Bahamian stromatolites (e.g. Stolz *et al.*, 2009), the relative importance of procaryotes vs. eucaryotes in stromatolite formation and the physiology of the phototrophs are not well known. Two previous studies provide some initial data. Kromkamp *et al.* (2007) and Perkins *et al.* (2007) used pulse amplitude modulated (PAM) fluorimetry to investigate the photophysiology of the cyanobacterial communities in classic mat type stromatolite samples. Standard rapid light curve (RLC) analysis in Kromkamp *et al.* (2007) gave proxy measurements of productivity [relative electron transport rate (rETR)] and the mechanisms behind photoactivation and inactivation upon sand burial. Perkins *et al.* (2007) described the ability of the cyanobacteria communities to withstand periods of natural sand burial (a common and potentially prolonged occurrence in the dynamic near shore sites where the stromatolites form) with rapid photosynthetic reactivation postburial upon exposure to low light and oxygen. These previous studies (Kromkamp *et al.*, 2007 and Perkins *et al.*, 2007) both acknowledged methodological problems associated with fluorescence signal from subsurface communities. Effectively, subsurface phototrophic cells representing the separation of taxa into distinct layers (see Stolz *et al.*, 2009 and also Table 1 and Fig. 1 in this study) result in data that are difficult to interpret because distances of cells from the fluorimeter and subsurface light environments are unknown (see Perkins *et al.*, 2010a for full details of this issue). This is analogous to measurements made on soft sediment biofilms with vertical migratory diatom cells (Kromkamp *et al.*, 1998; Serôdio and Catarino, 1999; Perkins *et al.*, 2002; Mouget *et al.*, 2008; Perkins *et al.*, 2010a).

To overcome errors associated with the presence of subsurface phototrophic communities in determining stromatolite productivity, this study used a mini-version of a Walz Imaging-PAM (Mini-I-PAM) to image cross sections of mats. Using this method, fluorescence measurements were made on individual layers (surface, 0–1 mm; shallow subsurface, 1–2 mm; or deep subsurface, 2–10 mm; see below), exposing each community or subcommunity to the same light environment during measurements and also maintaining each community at

**Table 1.** Mat types and phototrophic communities analysed in the present study, following terminology of Stolz *et al.* (2009) and Reid *et al.* (2000) and the dominant taxa within each community following Stolz *et al.* (2009)

| Sample type | Photosynthetic-community (cross-section layer) | Dominant phototropic taxa |
|---|---|---|
| Sample 1 | Type 1 – caramel surface | *Schizothrix gebeleinii* |
| | Type 3 – green subsurface | *S. gebeleinii*, *Solentia* spp., *Oscillatoria* sp |
| Sample 2 | Type 2 – bacterial biofilm with near-surface caramel cyanobacterial layer | Caramel layer: *S. gebeleinii* |
| Sample 3 | Near-surface cyanobacteria (Type 3 mat) | *Solentia* spp. and *Hyella* spp. – probably also *Microcoleus* and *Oscillatoria* |
| | Sub-surface green layer (Type 3 mat) | *Solentia* spp., *Hyella* spp., *Microcoleus chthonoplastes*, *Oscillatoria* sp., *S. gebeleinii* |
| Sample 4 | Pink Fuzz stalked diatoms | *Striatella unipunctata* |
| | Sub-surface caramel layer | *S. gebeleinii* |
| Sample 5 | Yellow fuzz stalked diatoms | *Licmophora remulus*, *Oscillatoria* sp. (potentially including other *Licmophora* spp., *S. unipunctata* and *Thalassionema* sp.) |
| | Sub-surface caramel layer | *S. gebeleinii* |
| Sample 6 – surface tube-dwelling diatoms with subsurface cyanobacteria | Surface diatom layer | Tube-dwelling diatoms (*Nitzschia* spp., *Navicula* spp. and *Amhipleura rutilans*) |
| | Sub-surface cyanobacteria – Type 3 mat | *Solentia* spp., *S. gebeleinii* |
| Sample 7 – coccoid pudding mats | Surface layer | *Phormidium* sp. and *S. gebeleinii* |
| | Subsurface green layer | Coccoid cyanobacteria (*Cyanothece*) |

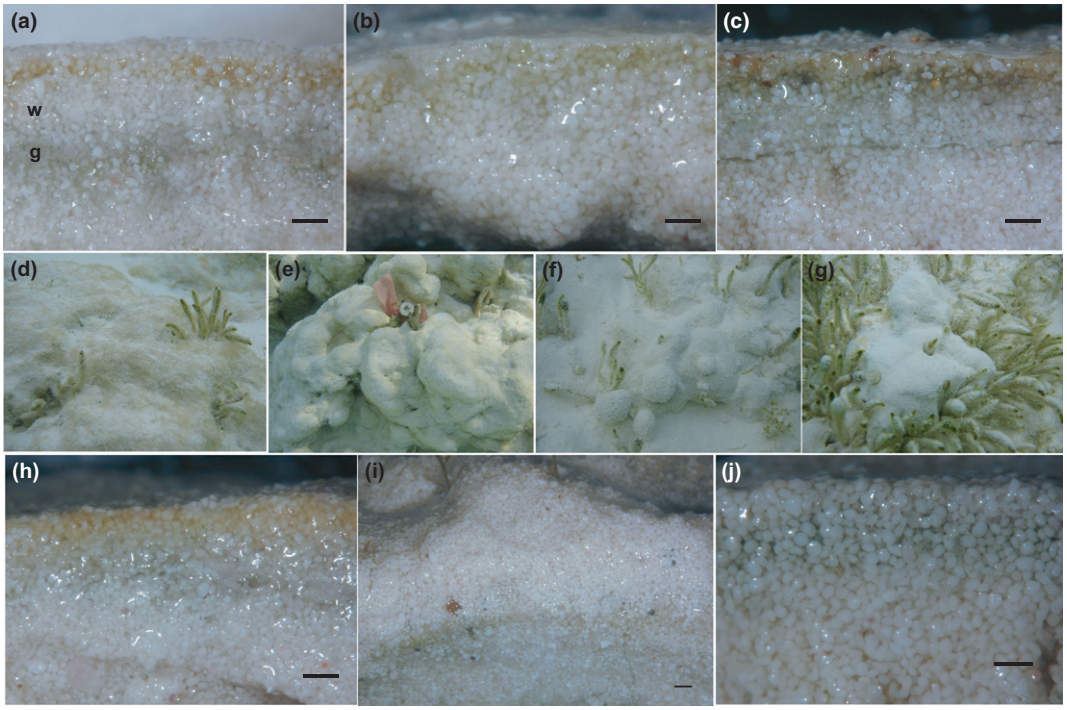


**Fig. 1.** Stromatolite phototrophic microbial communities at Highborne Cay, Bahamas. (a) Sample 1 – Type 1 mat of near surface *Schizothrix gebeleinii* community with underlying white (w) and green cyanobacteria community (g) layer; (b) Sample 2 – Type 2 mat comprising bacterial biofilm community with underlying *S. gebeleinii*; (c) Sample 3 – Type 3 mat, *Solentia* community; (d) Sample 4 – Pink fuzz, stalked diatom community; (e and h) Sample 5 – Yellow Fuzz, stalked diatom community with underlying *S. gebeleinii*; (f and i) Tube-dwelling diatom community with underlying *Solentia* and *S. gebeleinii*; (g and j) Pudding mat, *Phormidium* sp. and coccoid cyanobacterium community. Images a –c and h show the surface/near surface 'caramel layer' and images a, c, h–j show the subsurface 'green' sub-communities of cyanobacteria. a–c and h–j, cross-sections as observed under a dissecting microscope, d–g as they appear in the field. Scale bars are 1 mm.

the same distance from the fluorimeter, rather than having communities overlaying each other as in previous work (Kromkamp *et al.*, 2007; Perkins *et al.*, 2007). Although there will still be some element of subsurface signal because of the 3-D structure of the phototrophic layers within the sample, this error will be greatly reduced in comparison with measurements taken directly above the natural surface in which cell positions are unknown and the light levels apply only to the stromatolite surface. The attenuation of light within the stromatolite matrix can also be partly corrected for using the productivity proxy developed by Serôdio (2003) as explained in the methodology. The resultant data are therefore a far more accurate comparative measurement of community productivity than in previous work. However, it should be noted that the use of cross-sectioned samples exposes the sub-communities to the same light quality and quantity for the purpose of the comparative fluorescence measurements, but does not attempt to replicate the light fields experienced *in situ*. Use of the Mini-I-PAM also enabled replicate light curves to be performed simultaneously for each exposed community; thus, various eucaryote and procaryote communities were analysed at the same time.

This paper investigated the comparative productivity and photophysiology of the procaryotic and eucaryotic communities forming modern marine stromatolites at Highborne Cay. The overarching aim of the study was to determine the potential comparative photosynthetic activity of each procaryote phototrophic community in the different morphological mat types seen in the quasi-succession reported by Reid *et al.* (2000) and to compare these with the eucaryote communities described in Stolz *et al.* (2009). The study aimed to test the hypothesis that the cyanobacterial communities would have lower productivity and would be low light acclimated because of their subsurface locality within the stromatolite matrix, whereas surface eucaryote communities would have greater productivity and would be comparatively high light acclimated. In addition, we also tested the hypothesis that productivity would differ between stromatolite mat types defined within the 'quasi-succession' reported in literature (Reid *et al.*, 2000; Stolz *et al.*, 2009; Bowlin *et al.*, 2011).

## Materials and methods

### Sample collection

Samples were excised from stromatolites formed in shallow water on the eastern beach (Stromatolite Beach) of Highborne Cay, Exuma Sound (76°49′W, 24°43′N; Reid *et al.*, 1999) in July 2008. Samples were only collected during the morning (08:00–11:00). Samples were quickly placed onto a bed of site sand with overlying site seawater, inside a sealed opaque plastic container (and hence maintaining the sample in darkness). Samples were then quickly (within 20 min) returned to the laboratory onboard the R/V F.G. Walton Smith for fluorescence measurements. Samples were therefore effectively dark adapted for 20 min prior to measurements. On reaching the laboratory, samples were immediately cross-sectioned using a fine scalpel and fluorescence measurements were made (see below). Examination by light microscopy (e.g. Fig. 1) showed little to no damage to the 3-D structure of the stromatolite caused by cross sectioning. The study compared the productivity and photophysiology of the 13 procaryote and eucaryote phototrophic communities from seven sample types described in Table 1. Samples ($n = 7$, Table 1, column 1) were collected such that 10 individual sample replicates were obtained for each community ($n = 13$, Table 1, column 2).

### Community structure

All samples collected were analysed for community type, sub-community type and dominant taxa (Table 1) reported in the concomitant studies by Stolz *et al.* (2009) and Bowlin *et al.* (2011). The same nomenclature was used to describe communities and sub-communities of both procaryotes and eucaryotes and the same taxa are reported as dominant in these groupings. Thus, the sub-communities referred to in this study are indicative of those defined within the mat types referred to in previous literature, including the classic mat types of Reid *et al.* (2000).

### Fluorescence measurements

All fluorescence measurements were made using a Walz Mini-I-PAM fluorimeter and supporting Walz analysis software. Fluorimeter settings resulted in a low frequency nonactinic measuring beam and a 0.6 s saturating pulse of over 8000 μmol $m^{-2}$ $s^{-1}$ photosynthetically active radiation (PAR). Measurements of minimum or operational yield ($F_o$ in the dark and $F$ in the light respectively) and maximum fluorescence yield ($F_m$ in the dark and $F'_m$ in the light) were made, with calculation of PSII quantum efficiency following Genty *et al.* (1989):

$$F_v/F_m = (F_m - F_o)/F_m \text{ or } \Delta F/F'_m = (F'_m - F)/F'_m \quad (1)$$

for measurements in the dark and light, respectively.

Serôdio (2003) developed a chlorophyll fluorescence-based index to estimate productivity (where $E$ is the applied photosynthetically active radiation, PAR in μmol $m^{-2}$ $s^{-1}$):

$$P_{fluo} = E\frac{F_o}{F_{o,sed}}\Delta F/F'_m \quad (2)$$

When $F_o$ (the dark adapted minimum fluorescence yield) is corrected for background fluorescence from the sediment (effectively the autozero step in setting up the fluorimeter prior to use), this simplifies to:

$$P_{fluo} = F_o \cdot \text{rETR} \quad (3)$$

where rETR is the relative electron transport rate calculated as the product of $\Delta F/F'_m$ and E (Sakshaug *et al.*, 1997; Perkins *et al.*, 2006, 2010a). This results in a proxy ($P_{fluo}$ in Serôdio, 2003) that corrects for the vertical biomass profile and has been shown to have a linear correlation with oxygen evolution methods measuring productivity in sediment biofilms (Serôdio, 2003; Forster & Kromkamp, 2004; Lefebvre *et al.*, 2007; Serôdio *et al.*, 2007). The relative cell biomass/pigment content proportionally correlating with the $F_o$ signal is a form of correction for the light absorption coefficient ($a^*$) used in calculation of absolute electron transport rate. However, in this study, the term rETR is retained in favour over $P_{fluo}$ as the measurement made is still an electron transport rate partially corrected for light absorption, but is not an actual measurement of productivity such as oxygen evolution or carbon uptake. RLC were therefore constructed using rETR vs. $E$ (PAR) with 20-s-long incremental increases in PAR (0–380 μmol $m^{-2}$ $s^{-1}$). Light levels were calibrated in advance using a Licor cosine corrected quantum sensor. Light curve parameters of maximum electron transport rate ($rETR_{max}$), the light saturation coefficients ($E_k$ and $E_s$) and the initial slope of the light curve ($\alpha$) were solved using the model of Eilers & Peeters (1988) as explained in Perkins *et al.* (2006, 2010a, b). Curve fitting (using SIGMAPLOT v.15 software) was applied to all raw data and resultant light curve parameters were obtained from the full set of replicates ($n = 100$) and all fitted light curves were significant at $P < 0.001$. Note that to be able to calculate the product $F_o$·rETR and compare values between samples, the same fluorimeter settings (e.g. measuring light intensity and gain) were retained for all measurements.

Images of the cross-sectioned samples were focussed using the Mini-I-PAMs live video mode before switching to either red light (samples dominated by Cyanobacteria) or blue light (samples dominated by diatoms) illumination under the fluorescence imaging mode. It was interesting to note that samples analysed using both blue and red light separately, whether diatom or cyanobacteria dominated, showed no significant difference between each set of measurements. This was also noted in previous work by the authors (R.G. Perkins and J.C. Kromkamp, pers. obs.). Each community [illustrated in Fig. 1: surface diatom/cyanobacteria mixed community, surface cyanobacteria (typically the caramel layer) and subsurface cyanobacteria (green layer)], was imaged using 10 replicate polygons, carefully selected to enclose the community of interest. Note that subsurface images were only taken within 10 mm of the surface of the stromatolite to analyse communities within oxygenated zones reported in Stolz *et al.* (2009). The Mini-I-PAM processes the fluorescence yields detected within the selected polygon regions, hence performing separate light curves on each area. These measurements were repeated on 10 separate samples giving 10 pseudoreplicates within 10 true replicates, thus accounting for variability within samples and between samples. The data presented are therefore effectively mean values from 100 RLCs or the calculated values from the Eilers & Peeters (1988) curve fitting process when applied to all data for the 100 RLCs. The initial values of minimum and maximum fluorescence yields at the start of each light curve were used as proxy values of $F_o$ and $F_m$ [in all cases, these were the minimum and maximum yields, respectively, observed for each light curve set and indicated that chlororespiration (a form of oxygen-dependent electron transport) and state transitions had not depressed the $F'_m$ yield]. The initial value of $F_o$ was then used in the calculation of $P_{fluo}$ following Serôdio (2003) as described above (but retaining the nomenclature rETR), whilst $F_m$ was used in the calculation of the downregulation parameter of nonphotochemical quenching (NPQ) calculated as (e.g. see Perkins *et al.*, 2006, 2010a, b):

$$NPQ = (F_m - F'_m)/F'_m \quad (4)$$

## Results

### Stromatolite phototrophic communities

Table 1 presents the stromatolite phototrophic communities and sub-communities observed in the seven sample types investigated in this study. Nomenclature, except where stated, and taxa are as reported in the concomitant work by Stolz *et al.* (2009) and Bowlin *et al.* (2011). Images of the phototrophic communities are presented in Fig. 1. Sample 1, 2 and 3 (Fig. 1a–c) refer to the three 'classic' mat types of Reid *et al.* (2000). Figure 1a shows the Type 1 mat with the upper *S. gebeleinii* community and underlying mixed cyanobacteria. Figure 1b shows the Type 2 mat with upper bacterial biofilm and underlying *S. gebeleinii* community. Figure 1c shows the *Solentia* spp. community and underlying mixed cyanobacteria community. Figure 1d, the Pink Fuzz stalked diatom community sample, Fig. 1e and h, the Yellow Fuzz stalked diatom community, Fig. 1f and i, tube-dwelling diatom community and Fig. 1g and j, the 'Pudding mat' community, are the phototrophic 'nonclassic' mat type communities described in Table 1 and Stolz *et al.* (2009).

### 'Classic' mat types 1, 2 and 3

Type 1 stromatolite mat communities (Sample 1) showed a large difference between the caramel layer of *Schizothrix* at the surface and the subsurface Type 3 cyanobacteria community (Fig. 2). *Schizothrix* had higher rETR throughout the light curve and hence a higher $rETR_{max}$

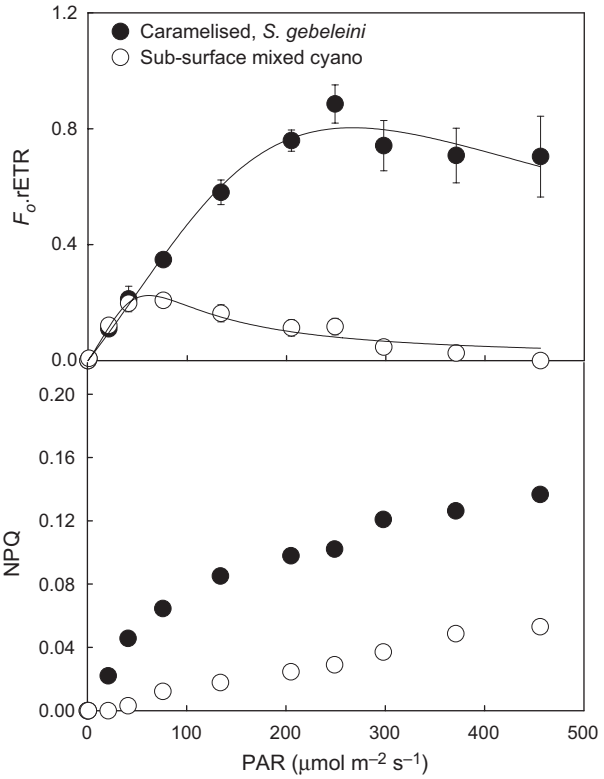


**Fig. 2.** Light response curves (upper panel) and NPQ induction during the same set of light curves (lower panel) for Type 1 Stromatolite mats comprising surface *Schizothrix gebeleiini* and sub-surface mixed cyanobacteria layer. All data mean ± SE from 10 replicate samples.

**Table 2.** Light curve parameters derived from the light curves in Figs 2 to 8 using the method of Eilers & Peeters, 1988. Derived light curve parameters a, b and c were all tested by regression curve fitting to the raw data (10 replicate light curves per sub-community) and were all significant at $P < 0.01$ (see Materials and methods for light curve methodology and curve fitting)

| Mat type | Dominant taxa | rETRmax (rel. units) | α (rel. units) | $E_k$ (μmol $m^{-2}$ $s^{-1}$ PAR) |
|---|---|---|---|---|
| Type 1 | Surf – *Schizothrix gebeleinii* | 0.80 | 0.004 | 180 |
| | Sub-surf – Schizothrix, *Solentia* and *Oscillatoria* spp. | 0.22 | 0.004 | 50 |
| Type 2 | Near Surf – *S. gebeleinii* | 0.35 | 0.001 | 350 |
| Type 3 | Near Surf – *Solentia* and *Hyella* spp. | 0.65 | 0.004 | 155 |
| | Sub-surf – mixed cyanobacteria | 0.70 | 0.005 | 140 |
| Stalked diatom mat (Pink Fuzz) | Surf – *Striatella unipunctata* | 0.34 | 0.005 | 70 |
| | Sub-surf – *S. gebeleinii* | 0.34 | 0.009 | 40 |
| Thrombolite Pink Fuzz | Surf – probable *Striatella unipunctata* | 0.40 | 0.004 | 100 |
| | Sub-surf – probable *S. gebeleinii* | 0.95 | 0.016 | 60 |
| Stalked diatom mat (Yellow Fuzz) | Surf – *Licmophora remulus* | 2.26 | 0.013 | 180 |
| | Sub-surf – *S. gebeleinii* | 0.77 | 0.009 | 90 |
| Tube diatom mats (Pustular blankets) | Surf – tube-dwelling diatoms | 1.40 | 0.019 | 75 |
| | Sub-surf – *Solentia* spp., *S. gebeleinii* | 0.81 | 0.013 | 65 |
| Coccoid pudding mats | Surf – *Phormidium* and *Schizothrix* | 1.02 | 0.009 | 120 |
| | Sub-surf – coccoid cyanobacteria | 0.81 | 0.004 | 205 |

Surf, surface layer of cells; Sub-surf, sub surface layer of cells; Near Surf, cells just below stromatolite surface (see Stolz *et al.*, 2009 for details). α, light use coefficient; $E_k$, light saturation coefficient (rounded to nearest 5 units).

and higher α (Table 2) than the subsurface community. Light saturation was higher for *Schizothrix* compared with the subsurface community, with an $E_k$ of 180 compared with 40 μmol $m^{-2}$ $s^{-1}$ PAR, respectively. In addition, *Schizothrix* showed only slight evidence for photoinhibition (i.e. a decrease in rETR at light levels above that for $rETR_{max}$), but comparatively high NPQ (Fig. 2) compared with the subsurface community which had clear photoinhibition and lower NPQ induction.

In contrast to Type 1 communities, Type 2 mats consisting of *Schizothrix* communities underlying a surface biofilm (Sample 2) showed a flatter light response curve with clear photoinhibition above $rETR_{max}$ (Fig. 3). Light curve parameters $rETR_{max}$ and α were lower (Table 2) for *Schizothrix* in Sample 2 mats, with an $E_k$ value calculated at 350 μmol $m^{-2}$ $s^{-1}$ PAR, appearing falsely high as this exceeds the saturation light level of 200 μmol $m^{-2}$ $s^{-1}$. The level of NPQ induction (Fig. 3) was similar to the surface layer of *Schizothrix* in Type 1 mats (Fig. 2), reaching a value of 0.12 by the end of the light response curve (compared to 0.16 for Type 1 *Schizothrix* community).

In Type 3 mats (Fig. 4), surface and subsurface *Solentia* communities showed almost identical light response curves. Light curves were intermediate between Type 1 and Type 2 mats as communities showed a comparatively high rETR throughout the light curve but with clear photoinhibition. In addition, NPQ induction was similar to levels observed in Type 1 and 2 mats (Fig. 4). $rETR_{max}$, α and $E_k$ values (Table 2) were similar for Type 3 communities of Sample 3 and were also similar to the Type 1 surface *Schizothrix* community. Overall, productivity decreased going from Type 1 to Type 2, as indicated by a

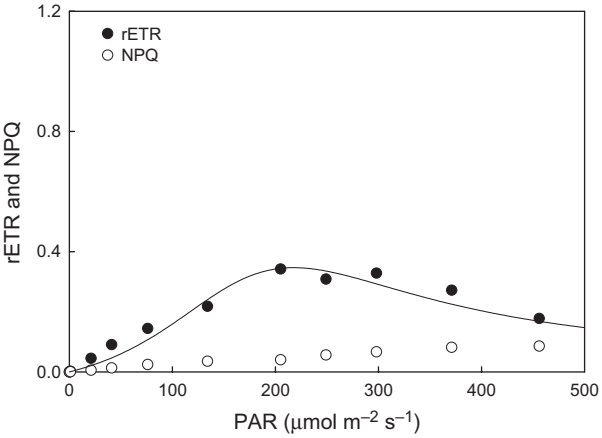


**Fig. 3.** Light response curves and NPQ induction during the same set of light curves for Type 2 Stromatolite mats comprising near surface *Schizothrix gebeleinii*. All data mean ± SE from 10 replicate samples.

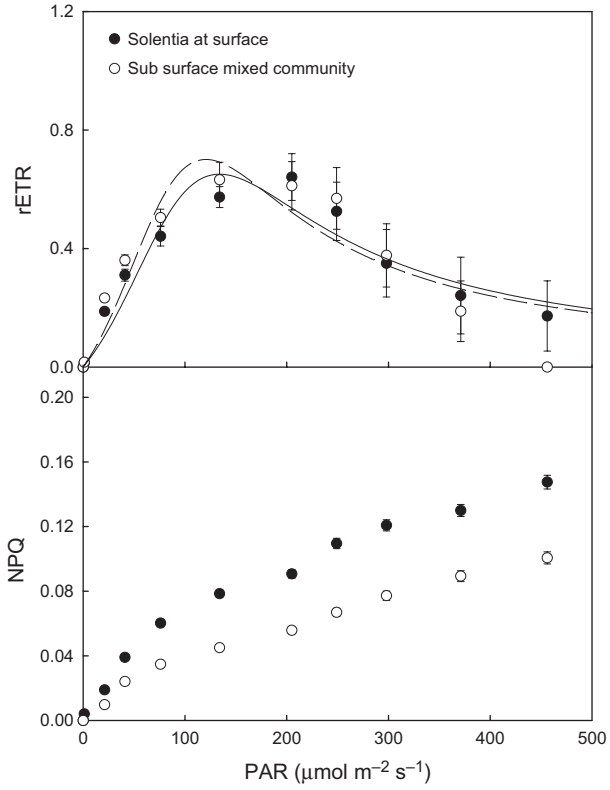


**Fig. 4.** Light response curves (upper panel) and NPQ induction during the same set of light curves (lower panel) for Type 3 Stromatolite mats comprising near surface *Solentia* sp. and sub-surface mixed cyanobacteria layer. All data mean ± SE from 10 replicate samples.

comparative reduction in both $rETR_{max}$, and then increased again in Type 3 mats.

## 'Nonclassic' mat types with eucaryote communities

The two stalked diatom stromatolite mat types, Pink Fuzz (Sample 4) and Yellow Fuzz (Sample 5) dominated by *Striatella* sp. or *Licmophora* sp. respectively, and both overlaying *Schizothrix*, showed distinctly different productivity and downregulation (Fig. 5). Surprisingly, the surface *Striatella* community (Sample 4, Pink Fuzz) had a light response curve almost identical to the subsurface *Schizothrix* of Sample 4 with similar $rETR_{max}$, $\alpha$ and $E_k$ values (Table 2). In comparison, *Licmophora* (Sample 5, Yellow Fuzz) had the highest values of rETR throughout the light response curve and hence the highest $rETR_{max}$ and $\alpha$ of any phototrophic community. In addition, the subsurface *Schizothrix* underlying *Licmophora* had a higher $rETR_{max}$ and $\alpha$ than the *Schizothrix* community underlying *Striatella*, as well as being higher than the *Striatella* itself. The level of NPQ induction for both *Striatella* and the subsurface *Schizothrix* of the Pink Fuzz community (Sample 4) was greater than the two communities of Yellow Fuzz (Fig. 6) and also saturated by the end of the light curve. These were the only communities to show saturation of NPQ induction.

Pink Fuzz and Yellow Fuzz surface eucaryote communities on nearby Thrombolites were additionally compared with those on Stromatolites. Interestingly, Pink Fuzz on the nearby thrombolite samples showed a very different pattern to Pink Fuzz on stromatolite samples (Fig. 6) despite the hypothesis that these were the same community types (verified by light microscopy). Surface stalked diatoms on thrombolites, dominated by *Striatella* sp., had a similar light curve and level of NPQ induction as the comparable layer on the stromatolite surface, hence showing similar $rETR_{max}$, $\alpha$ and $E_k$ (Table 2). The thrombolite subsurface cyanobacteria dominated by *Schizothrix*, underlying the stalked diatoms, had higher $rETR_{max}$, $\alpha$ and $E_k$ than the diatoms (Fig. 6, Table 2), with values similar to those of the subsurface *Schizothrix* layer in the stromatolite Yellow Fuzz community (Fig. 5, Table 2) despite having a similar level of NPQ induction to the surface stalked diatoms.

Tube-dwelling diatoms at the surface of stromatolite sample 6 were a highly productive community with high rETR, showing no downregulation in rETR above $rETR_{max}$. The light curve for the subsurface Type 3 cyanobacterial community saturated with a comparatively high $rETR_{max}$ relative to the majority of cyanobacteria subsurface layers (Fig. 7 and Table 2). The subsurface Type 3 cyanobacteria community showed downregulation in rETR at high irradiance despite a similar level of NPQ induction as the surface diatoms, with neither community showing saturation of NPQ induction (Fig. 7). In general, with the exception of the *Striatella* community in Pink Fuzz (Sample 4), the eucaryote diatom-dominated communities and the associated subsurface cyanobacteria showed high productivity.

The final community studied was the relatively soft coccoid pudding mats (Sample 7) formed on the surface of some stromatolites. This community is composed of a surface layer of *Phormidium* and *Schizothrix*, with a subsurface layer of coccoid cells tentatively identified as *Cyanothece* (Stolz *et al.*, 2009). The two layers showed similar productivity (Fig. 8), although surprisingly the subsurface coccoid layer had higher $rETR_{max}$ and $\alpha$ than the surface layer (Table 2). Both layers had comparatively high productivity compared with the cyanobacterial communities in other samples and both communities showed typical patterns of NPQ induction which did not saturate by the end of the light curve (Fig. 8). Apart from the *Striatella* Pink Fuzz community (see above), the coccoid community was the only sample in which the

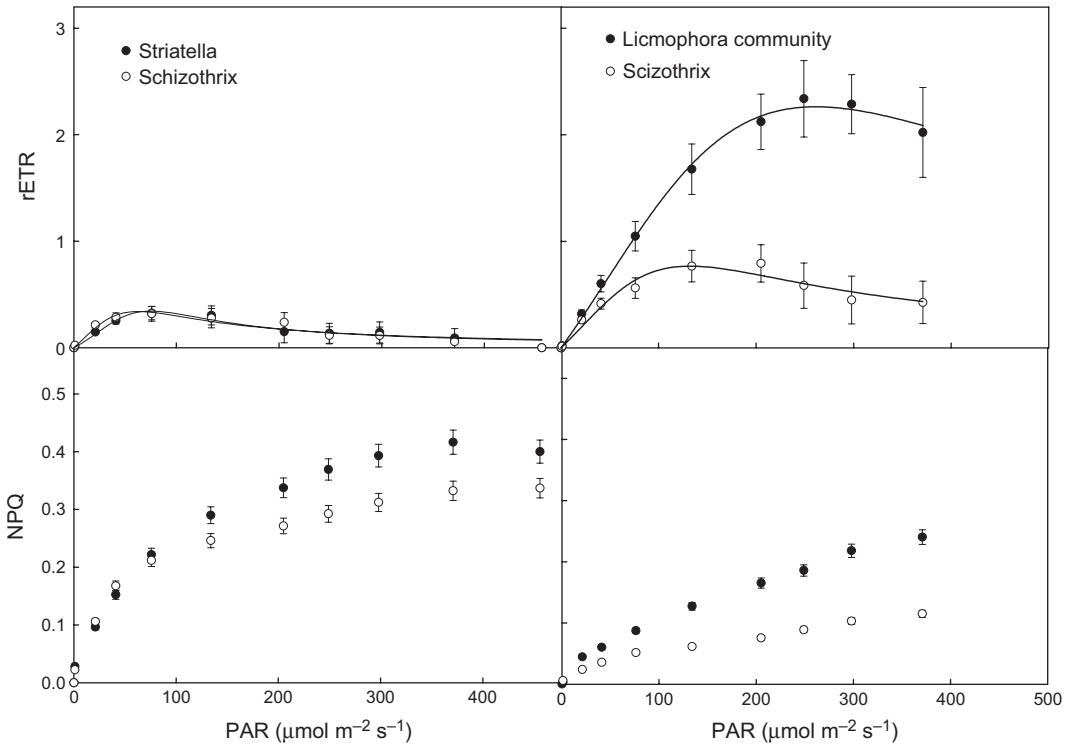


**Fig. 5.** Light response curves (upper panels) and NPQ induction during the same set of light curves (lower panels) for stalked diatom sub-communities overlying *Schizothrix gebeleinii*. Left-hand panels refer to 'Pink Fuzz' dominated by *Striatella* sp. and right-hand panels refer to 'Yellow Fuzz' dominated by *Licmophora* sp. All data mean ± SE from 10 replicate samples.

subsurface cyanobacterial productivity exceeded the productivity of the surface community.

## Discussion

Photosynthetic activity varied greatly between sub-communities of both procaryotic and eucaryotic autotrophs in the stromatolite samples collected at Highborne Cay. Productivity was measured for the sub-communities previously defining the succession of classical stromatolite mat types (Reid *et al.*, 2000; Stolz *et al.*, 2009; Bowlin *et al.*, 2011), and hence, the sub-communities referred to and used also to refer to the stage of this succession. With regard to the procaryotic cyanobacteria, comparative productivity was higher for Type 1 *Schizothrix* communities (Sample 1) than *Schizothrix* underlying Type 2 bacterial-dominated biofilms (Sample 2). Productivity was again higher in Type 3 mats (Sample 3). The data in this study suggest a productive community in Type 1 mats is followed by a less productive one in Type 2 mats, where cyanobacteria would be less active in stromatolite accretion, and finally another productive cyanobacterial climax community in Type 3 mats. Reid *et al.* (2000) hypothesized a dynamic balance between periods of sediment accretion and intervals when no accretion occurred with a mat type progression from Type 1 to Type 2 and thence to Type 3 as a form of climax community. This progression was thought to be dependent upon a pause in sediment accretion, presumably resulting from changes in hydrodynamic forces (wave and storm events) with corresponding changes in sediment supply (Reid *et al.*, 2000; Stolz *et al.*, 2009). The data in this study therefore show a pattern in productivity which parallels the pattern in stromatolite sediment accretion suggested by Reid *et al.* (2000) It should be noted that these data for productivity are comparative and not quantitative. As samples were cross-sectioned, it could be argued that enhanced exposure to oxygen may change absolute values of productivity, and the authors do not dispute this. However, this would be highly unlikely to change the comparative patterns in data observed for either the productivity proxy or the data on photoacclimation.

### Comparative productivity

Within Type 1 mats, the surface caramel layer of *S. gebeleinii* had a comparatively high $rETR_{max}$ of 0.80 compared with the subsurface Type 3 community of *Schizothrix*, *Solentia* and *Oscillatoria* spp. ($rETR_{max}$ of 0.22). This suggests greater primary productivity near the surface and

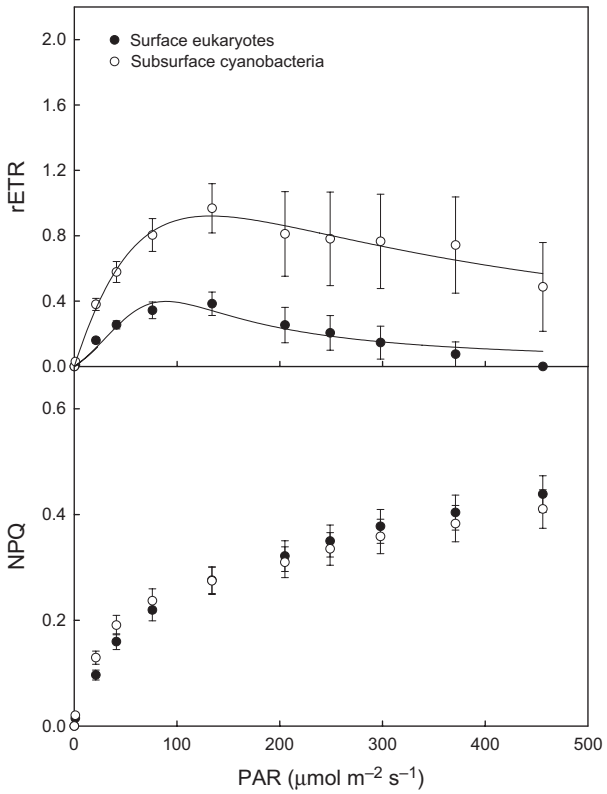


**Fig. 6.** Light response curves (upper panel) and NPQ induction during the same set of light curves (lower panel) for stalked diatom sub-communities (thought to be *Striatella* sp.) overlying cyanobacteria sub-community layer (thought to be *Schizothrix gebeleinii*) on thrombolite samples. This is the thrombolite 'Pink Fuzz' equivalent to the Stromatolite samples in Fig. 5. All data mean ± SE from 10 replicate samples.

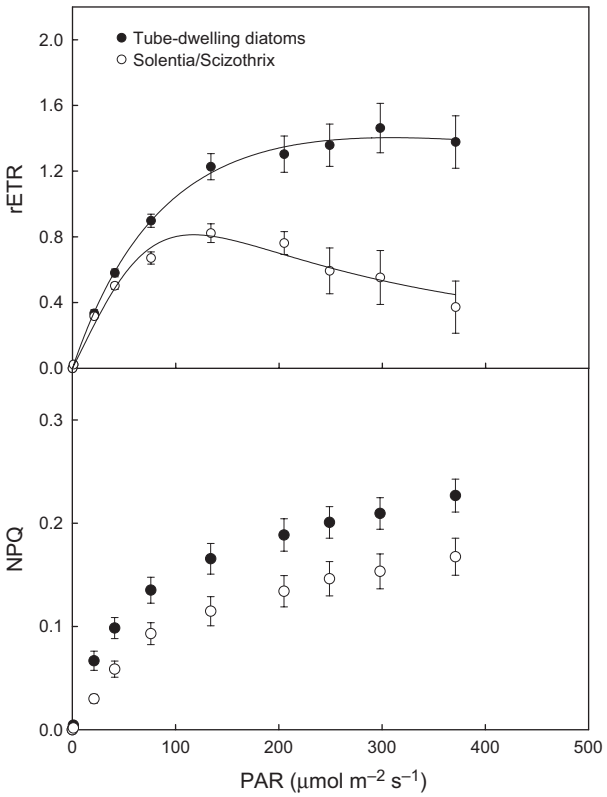


**Fig. 7.** Light response curves (upper panel) and NPQ induction during the same set of light curves (lower panel) for tube-dwelling diatom sub-communities overlying *Solentia* sp./*Schizothrix gebeleinii*. All data mean ± SE from 10 replicate samples.

hence a potential for a greater role in polymer production and a potential for sediment trapping. Type 1 mats are typified by pioneer filamentous cyanobacteria, *Schizothrix*, and dominate during periods of rapid sedimentation (Reid *et al.*, 2000; Visscher *et al.*, 2000; Riding *et al.* 2000; Stolz *et al.*, 2009); hence a high rETR indicating high productivity would be expected. Such a high level of productivity would also be required to produce the large amounts of extracellular polymeric substances (EPS) as reported for *Schizothrix* within Type 1 mats (Stolz *et al.*, 2009) which is of high importance in defining its role in sediment binding.

In contrast to Type 1 mats, the Type 2 mat with a near-surface layer of *Schizothrix* showed a lower $rETR_{max}$ of 0.35 rel. units. Type 2 biofilms (overlying the Type 1 community in Sample 2) are thought to form during a pause in sediment accretion and represent the stage at which bacterial mineralization of biofilm polymer leads to formation of a micritic crust (Reid *et al.*, 2000). This period is not favourable for cyanobacterial photosynthetic activity, leading to lower productivity. It is possible that the bacterial activity within the biofilm may reduce the amount of oxygen available to the cyanobacteria potentially inhibiting oxygen-dependent electron transport; this is consistent with previous findings that oxygen is essential for cyanobacterial photosynthetic reactivation postburial (Perkins *et al.*, 2007).

As the pause in sedimentation increases in duration, the cyanobacterial community evolves into climax Type 3 community dominated by *Solentia* (which bores into the sand grains increasing matrix stability) and *Hyella,* sometimes with a subsurface Type 3 cyanobacterial community (Reid *et al.*, 2000; Stolz *et al.*, 2009). Both layers in the Type 3 mats (Sample 3) had higher productivity than the Type 1 community underlying the Type 2 biofilms (Sample 2) with $rETR_{max}$ of 0.65 and 0.70 rel. units for the surface and subsurface communities, respectively. This would be expected if the climax community had effectively moved through a less favourable period for photosynthetic activity into a period when cyanobacterial photosynthetic activity increased. Type 3 mats consist of a climax community comprising microboring of sediment

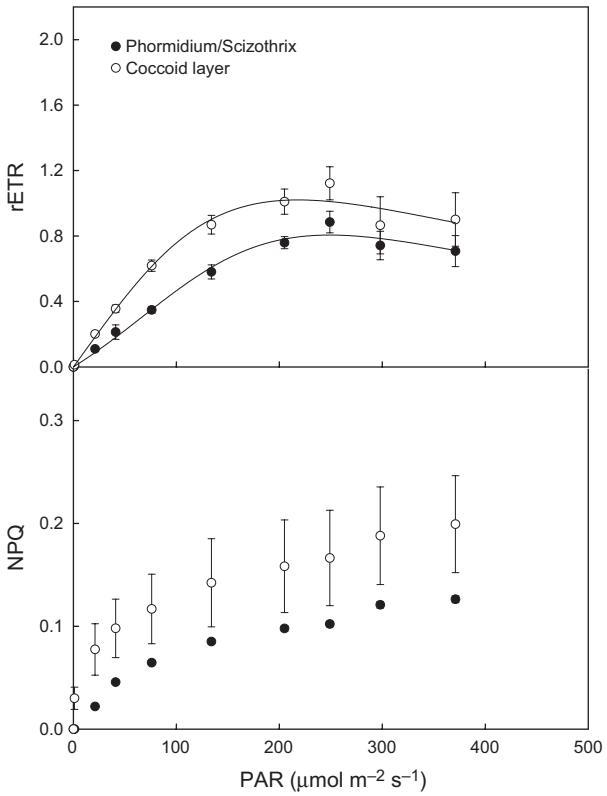


**Fig. 8.** Light response curves (upper panel) and NPQ induction during the same set of light curves (lower panel) for 'coccoid pudding mats' thought to be comprised of *Phormidium* sp. and *Schizothrix gebeleinii* overlying a coccoid cell layer possibly *Cyanothece* sp. All data mean ± SE from 10 replicate samples.

grains by *Solentia* and potentially an increase in *Schizothrix* biomass (Bowlin *et al.*, 2011). However, analysis using oxygen microelectrodes by Stolz *et al.* (2009) indicated broadly similar oxygen profiles for the three 'classic' mat types but with an oxygen maximum for a Type 2 mat approximately double that for Type 1 and 3 mats. The higher oxygen in the Type 2 mat suggests greater photosynthetic oxygen evolution despite a concomitantly higher level of bacterial respiration which would be expected to reduce the oxygen detected in the Type 2 profile (Stolz *et al.*, 2009). One explanation for the higher oxygen in Type 2 mats might be a lower oxygen diffusivity because of inhibition by the micritic layer leading to oxygen accumulation. Unfortunately, EPS data for Type 1 and 2 mats in the same study were pooled, although a higher percentage as well as absolute amount of colloidal low molecular weight polymer (cLMW) was observed in Type 3 mats compared with the pooled Type 1 and 2 mats. Comparatively greater cLMW production would support a higher rate of photosynthetic productivity (Smith & Underwood, 1998; Decho, 2000; Perkins *et al.*, 2001; Underwood, 2001).

Bowlin *et al.* (2011) reported that as the period of low sedimentation persists, or in the absence of frequent burial, eucaryotic surface colonizers (stalked and tube-dwelling diatoms) develop on the stromatolite surface. In this study, there was a large difference in the productivity of the two stalked diatom communities with *Licmophora* of Yellow Fuzz having a higher $rETR_{max}$ than *Striatella* of Pink fuzz (2.26 compared with 0.34 rel. units). Subsurface layers of *Schizothrix* underlying the Pink and Yellow Fuzz also showed differences in productivity with $rETR_{max}$ of 0.77 rel. units under *Licmophora* compared with 0.34 rel. units under *Striatella*. The different surface communities therefore not only differ in their own productivity, but also appear to have different affects on the productivity of the subsurface cyanobacteria. It is likely that this would have implications on sub-community function regarding sediment binding and accretion.

When comparing thrombolite and stromatolite phototrophic communities, differences in photophysiology were observed despite the communities being hypothesized to be comprised of the same taxa. Pink Fuzz on thrombolite samples had a low $rETR_{max}$ (0.40 rel. units) similar to the Pink Fuzz on the stromatolite but the subsurface layer of cyanobacteria, presumably *Schizothrix*, was potentially far more productive with an $rETR_{max}$ of 0.95. This difference for the subsurface *Schizothrix* suggests two possibilities: firstly, subtle differences in the depth of the subsurface cyanobacterial layer in the stromatolite fabric result in different states of photoacclimation (high or low light states), or secondly, other unknown factors lead to higher rates of productivity, suggesting more favourable conditions for the *Schizothrix* subsurface compared to *Licmophora* and within the Thrombolite structure.

The potential productivity of the Stromatolite tube-dwelling diatom community was intermediate between the *Licmophora* and *Striatella* communities, with an $rETR_{max}$ of 1.4. This $rETR_{max}$ indicates higher productivity than the procaryote autotrophs, but considerably lower than the *Licmophora* community. The subsurface layer of *Schizothrix* under the tube-dwelling diatoms showed a relatively high $rETR_{max}$ of 0.81. Thus, in two of three cases, the surface eucaryote potential productivity was significantly higher than that of the underlying cyanobacteria layer, but in all cases the cyanobacteria were photosynthetically active with reasonably high $rETR_{max}$.

The relevance of the coccoid pudding mat community in stromatolite formation is not known. However, this mat type was noted as an exception in that the subsurface coccoid layer (tentatively identified as *Cyanothece*) had a higher $rETR_{max}$ and $\alpha$ compared with the *Schizothrix*/*Phormidium* community ($rETR_{max}$ of 1.02 rel. units compared with 0.81, $\alpha$ of 0.009 compared to 0.004 rel. units).

The high rETRmax suggests that the coccoid cells are potentially highly active with respect to productivity within the subsurface communities. This is in agreement with the high proportion of cLMW polymer, the high subsurface Chl *a* content and the penetration of oxygen to 24 mm (the deepest profile of all mat types) reported in Stolz *et al.* (2009).

In general, comparative productivity data based on the $rETR_{max}$ proxy suggest cyanobacterial communities have comparatively lower productivity than surface eucaryotic communities dominated by stalked and tube-dwelling diatoms; an exception is the coccoid cyanobacteria community of the pudding mats, with $rETR_{max}$ equivalent to the diatoms. These productivity patterns are supported by the oxygen profiles and the polymer data of Stolz *et al.* (2009).

### Photoacclimation and downregulation

Comparison of the RLC parameters $rETR_{max}$, $\alpha$ and $E_k$ enable states of photoacclimation, for example adaptation to high light or low light (in relative terms), to be compared between samples. High $rETR_{max}$ and $E_k$ with relatively low $\alpha$ indicates high light acclimation and vice versa for low light acclimation. However, in this study the product $F_o$·rETR was used to estimate productivity to reduce the influence of light attenuation in the cross-sectioned sample. As a result, any differences in photoacclimation need to be treated with caution. Procaryote sub-communities showed no consistent patterns in photoacclimation state. For example, surface caramel *Schizothrix* had a similar $\alpha$ to the subsurface Type 3 community, although the $rETR_{max}$ and $E_k$ were higher at the surface. Type 3 mat communities showed similar values of $rETR_{max}$, $\alpha$ and $E_k$ to the *Schizothrix* caramel layer, despite variation of the communities with depth. Type 3 mats near the stromatolite surface had low $\alpha$ and $E_k$, but a relatively high $rETR_{max}$. In contrast the eucaryote diatom communities showed higher $\alpha$ and $rETR_{max}$ compared with the cyanobacteria communities, despite having $E_k$ values of a similar magnitude. This would suggest a greater potential productivity of the eucaryotes but otherwise no difference in light acclimation state. Downregulation through photoprotection was suggested for the surface/near-surface *Schizothrix* communities with high carotenoid content being observed and a high sensitivity to light under a light microscope reported (Stolz *et al.*, 2009). Also the tube-dwelling diatoms were reported by Stolz *et al.* (2009) as showing sensitivity to light, but in this study they showed comparatively high $rETR_{max}$, $\alpha$, $E_k$ and levels of NPQ which were similar to those of the stalked diatom communities.

Downregulation through induction of NPQ was observed to increase as the light level incrementally increased in RLCs for all samples, however the magnitude of this increase varied. For subsurface sub-communities of cyanobacteria the level of NPQ induction was similar reaching values of around 0.1–0.16 by the end of the RLC, except for the Type 1 mixed community which induced NPQ to a lower extent (approximately 0.04 by the end of the RLC) and the *Schizothrix* layer underlying the Pink Fuzz on both stromatolites and thrombolites which had higher levels of NPQ (0.3 and 0.4 for stromatolite and thrombolite sub-communities, respectively). This suggests a relatively constant level of photoacclimation indicated by the ability to induce NPQ. The relatively high level of NPQ for the *Schizothrix* layer under the two Pink Fuzz communities is surprising, but it was noted that the level of NPQ induction of the surface Pink Fuzz (*Striatella* for the stromatolite samples and presumably the same dominant taxa at least for the thrombolites) was also the same (0.4 by the end of the RLCs for both stromatolite and thrombolite sub-communities). Overall, the Pink Fuzz stalked diatom/*Schizothrix* community had lower productivity (see above) and higher levels of downregulation when compared with all other sub-communities, suggesting low light acclimation. In all cases the more productive eucaryote communities dominated by stalked diatoms and tube-dwelling diatoms showed higher levels of NPQ induction compared with the cyanobacteria, suggesting a better ability to cope with the relatively higher light level at the stromatolite surface.

## Conclusions

Overall, this study has shown differences in comparative productivity in photosynthetic sub-communities within stromatolite mat types. Broadly speaking, the cyanobacterial communities typical of 'classic' mat types had lower productivity, without showing clear patterns in photoacclimation in the form of high or low light acclimation. Productivity of the eucaryote, principally diatom dominated, communities was mostly higher, except in the stalked diatom community dominated by *Striatella*, probably resulting from the low Chl *a* content of this sub-community reported by Stolz *et al.* (2009). The patterns in comparative productivity correlate well with the quasi-succession between the morphological phenotypes (mat types) reported by Reid *et al.* (2000) and defined with respect to community by Stolz *et al.* (2009). A photosynthetically active cyanobacterial community in Type 1 mats is followed by a potentially less productive sub-community underlying Type 2 mats, when bacterial mineralization activity is high. This in turn is followed by a more productive mixed cyanobacteria climax community in Type 3 mats. In the longer term, surface eucaryote sub-communities, dominated by diatoms, form mixed communities which have compara-

tively higher productivity than the cyanobacterial subcommunities.

## Acknowledgements

Many thanks to the ship's crew and fellow scientists on board the RV 'F.G. Walton Smith' for their support. This study was funded by the U.S. National Science Foundation. R.G.P. was in part supported by a Cardiff University research travel grant. J.-L.M. was in part funded by the Université du Maine and the same NSF grant. Part of this work was made possible through a Schure-Beijering Popping fund grant to J.C.K. Thanks also to Walz, Germany, for the kind loan of the Mini-I PAM fluorimeter to carry out this research. This is RIBS publication No. 65.

## References

Bowlin EM, Klaus J, Andres MS, Custals L & Reid RP (2011) Environmental controls on microbial community cycling in modern marine stromatolites. *Sediment Geol* (available online) **263**: 45–55.

Decho AW (2000) Exopolymer microdomains as a structuring agent for heterogeneity within biofilms. *Microbial Sediments* (Riding RE & Awramik SM, eds), pp. 9–15. Springer, UK.

Eilers PCH & Peeters JCH (1988) A model for the relationship between light intensity and the rate of photosynthesis in phytoplankton. *Ecol Model* **42**: 199–215.

Forster RM & Kromkamp JC (2004) Modelling the effects of chlorophyll fluorescence from subsurface layers on photosynthetic efficiency measurement in microphytobenthic algae. *Mar Ecol Prog Ser* **284**: 9–22.

Genty B, Briantais JM & Baker NR (1989) The relationship between the quantum yield of photosynthetic electron transport and quenching of chlorophyll fluorescence. *Biochim Biophys Acta* **990**: 87–92.

Kromkamp J, Barranguet C, Peene J (1998) Determination of microphytobenthos PSII quantum efficiency and photosynthetic activity by means of variable chlorophyll fluorescence. *Mar Ecol Prog Ser* **162**: 45–55.

Kromkamp JC, Perkins RG, Dijkman N, Consalvey M, Andres M & Reid RP (2007) Resistance to burial of cyanobacteria in stromatolites. *Aquat Microb Ecol* **48**: 123–130.

Lefebvre S, Mouget J-L, Loret P & Tremblin G (2007) Comparison between fluorimetry and oxymetry techniques to measure photosynthesis in the diatom *Skeletonema costatum* cultivated under simulated seasonal conditions. *J Photochem Photobiol B Biol* **86**: 131–139.

Mouget J-L, Perkins RG, Consalvey M & Lefebvre S (2008) Migration or photoacclimation to prevent photoinhibition and UV-B damage in marine microphytobenthic communities. *Aquat Microb Ecol* **52**: 223–232.

Perkins RG, Underwood GJC, Brotas V, Jesus B, Ribeiro L & Snow G (2001) *In situ* microphytobenthic primary production during low tide emersion in the Tagus estuary, Portugal: production rates, carbon partitioning and vertical migration. *Mar Ecol Prog Ser* **223**: 101–112.

Perkins RG, Oxborough K, Hanlon ARM, Underwood GJC & Baker NR (2002) Can chlorophyll fluorescence be used to estimate the rate of photosynthetic electron transport within microphytobenthic biofilms? *Mar Ecol Prog Ser* **228**: 47–56.

Perkins RG, Mouget J-L, Lefebvre S & Lavaud J (2006) Light response curve methodology and possible implications in the application of chlorophyll fluorescence to benthic diatoms. *Mar Biol* **149**: 703–712.

Perkins RG, Kromkamp J & Reid RP (2007) How do stromatolite photosynthetic communities tolerate natural sand burial events? The roles of light and oxygen in photochemical reactivation. *Mar Ecol Prog Ser* **349**: 23–32.

Perkins RG, Kromkamp JC, Serôdio J, Lavaud J, Jesus B, Mouget J-L *et al.* (2010a) The application of variable chlorophyll fluorescence to microphytobenthic biofilms. In Chlorophyll a fluorescence in aquatic sciences: methods and applications. *Developments in Applied Phycology*, vol. 4 (Suggett D, Prasil O & Borowitzka M, eds), pp. 237–275. Springer, London.

Perkins RG, Lavaud J, Serôdio J, Mouget J-L, Cartaxana P, Rosa P *et al.* (2010b) Vertical cell movement is a primary response of intertidal benthic biofilms to increasing light dose. *Mar Ecol Prog Ser* **416**: 93–103.

Reid RP, Macintyre IG, Steneck RS, Browne KM & Miller TE (1995) Stromatolites in the Exuma Cays, Bahamas: uncommonly common. *Facies* **33**: 1–18.

Reid RP, Macintyre IG & Steneck RS (1999) A microbialite/algal ridge fringing reef complex, Highborne Cay, Bahamas. *Atoll Res Bull* **466**: 1–18.

Reid RP, Visscher PT, Decho AW, Stolz J, Bebout BM, Dupraz C *et al.* (2000) The role of microbes in accretion, lamination and early lithification of modern marine stromatolites. *Nature* **406**: 989–992.

Riding R (2000) Microbial carbonates: the geological record of calcified bacterial-algal mats and biofilms. *Sedimentology* **47**: 179–214.

Sakshaug E, Bricaud A, Dandonneau Y, Falkowski P, Keifer D, Legendre L *et al.* (1997) Parameters of photosynthesis: definitions, theory and interpretation of results. *J Plankton Res* **19**: 1637–1670.

Serôdio J (2003) A chlorophyll fluorescence index to estimate short-term rates of photosynthesis by intertidal microphytobenthos. *J Phycol* **39**: 33–46.

Serôdio J, Vieira S & Barroso F (2007) Relationship of variable chlorophyll fluorescence indices to photosynthetic rates in microphytobenthos. *Aquat Microb Ecol* **49**: 71–85.

Shapiro RS (2000) A comment on the systematic confusion of thrombolites. *Palaios* **15**: 166–169.

Smith DJ & Underwood GJC (1998) Exoplymer production by intertidal epipelic diatoms. *Limnol Oceanogr* **43**: 1578–1591.

Stolz JF, Reid RP, Visscher PT, Decho AW, Norman RS, Aspden RJ *et al.* (2009) The microbial communities of the

modern marine stromatolites at Highborne Cay, Bahamas. *Atoll Res Bull* **567**: 1–29.

Underwood GJC (2001) "Microphytobenthos". *Encyclopedia of Ocean Sciences* (Steele J, Thorpe S & Turekian K, eds), pp. 1770–1777. Academic Press, London.

Visscher PT, Reid RP & Bebout BM (2000) Microscale observations of sulfate reduction: correlation of microbial activity with lithified micritic laminae in modern marine stromatolites. *Geology* **28**: 919–922.